Chemical Science

Accepted Manuscript

This article can be cited before page numbers have been issued, to do this please use: R. Zhang, X. Lyu, T. Li and A. J. L. Grimaud, *Chem. Sci.*, 2025, DOI: 10.1039/D5SC03012A.

View Article Online
DOI: 10.1039/D5SC03012A

Optimizing semi-hydrogenation of unsaturated hydrocarbons by electrolyte engineering approach

Rongyu Zhang,[1] Xingyi Lyu,[2,3] Tao Li[2,3] and Alexis Grimaud[1]

[1]Department of Chemistry, Boston College, Chestnut Hill, MA, USA, 02467

[2]Department of Chemistry and Biochemistry, Northern Illinois University, DeKalb, IL, 60115

[3]X-ray Science Division, Argonne National Laboratory, Lemont, IL, 60439

Corresponding authors: alexis.grimaud@bc.edu

Abstract

Electrochemical hydrogenation of unsaturated hydrocarbons, when powered by renewables, represents a unique opportunity to substitute current energy-intensive synthetic routes. Modulation of adsorption energies of the organic substrate and key intermediates of the reaction is critical for fine tuning of the yield, selectivity and kinetics of the reaction. Interestingly, mounting evidences exist regarding the role of electrolyte composition on the outcome of semi-hydrogenation reactions. Nevertheless, electrolyte optimization is a complex task, owing to its hybrid nature. Indeed, it is composed of water serving as proton source, an organic solvent necessary to dissolve the organic substrate and a conducting salt. Herein, we demonstrate that varying conducting salt and organic solvent have a dramatic impact on the outcomes of semi-hydrogenation of alkynes. By varying salt and water concentration, we demonstrate that water does not serve as proton source, and instead addition of an acid is necessary.

View Article Online
DOI: 10.1039/D5SC03012A

While increasing acid concentration increases the yield of the reaction, at too large concentrations hydrogen evolution reaction becomes predominant. Furthermore, combining electrochemical measurements with spectroscopic techniques including Fourier transform infrared (FTIR) spectroscopy and small angle X-ray spectroscopy (SAXS), we demonstrate that the electrolyte solvation structure dramatically impacts the yield of the reaction. Organic solvents weakly interacting with water, including acetonitrile, form aqueous nanoheterogeneities that prevent the organic substrate from accessing the catalyst interface and thus lead to limited yields. Instead, solvents such as dimethylformamide form homogeneous mixtures with which all reactants can access the interface, leading to yields greater than 80% for optimized compositions.

Introduction

Organic electrosynthesis has recently gained renewed attention as, when powered by renewables, it is regarded as a more environmentally friendly approach compared to energy-intensive routes utilizing redox reagents.[1-4] This is specifically the case for hydrogenation reactions, for which conventional synthesis routes require harsh conditions,[5] including high temperature[6] or high pressure,[7, 8] and complex procedures to achieve good yield and conversion. So far, a variety of electrosynthesis strategies have been developed and employed for efficient and selective hydrogenation of unsaturated organic compounds.[9-14] Most efforts have been devoted to designing better electrocatalysts with the aim of enhancing the reaction rate and selectivity by controlling the intermediates forming on the surface of the catalyst.[12, 15, 16] Nevertheless, numerous results point to the critical role played by the electrolyte optimization on the outcome of hydrogenation reactions, more specifically its composition.[17, 18]

As commonly believed, hydrogenation reactions require the formation of H*

View Article Online
DOI: 10.1039/D5SC03012A

intermediate following the electrochemical reduction of water or protons, this intermediate being transferred to the unsaturated hydrocarbon (alkyne or alkene) or involved in a hydration-dehalogenation process.[10, 19-21] Nevertheless, when targeting the hydration of insoluble organic substrates, water that acts as proton source must be mixed with an organic solvent to solubilize the organic substrate, forming a so-called hybrid electrolyte.[22] Hybrid electrolytes have thus been used in various hydrogenation reactions, including the hydrogenation of alkynes into alkenes or the hydrogenation of halogenated alkyls, using solvents including acetonitrile (ACN), dimethylformamide (DMF), or acetone, among others.[23-25]

Past studies have shown that the composition and structure of hybrid electrolytes strongly impact the water reactivity at electrochemical interface, with the hydrogen evolution reaction (HER) competing with hydrogenation reactions in hybrid electrolytes being highly sensitive to the organic solvent.[26, 27] This effect is rooted in the role played by short-range interactions, including ions-water, water-water and organic solvent-water, which drastically modifies the solvation structure and the dynamics of hybrid electrolytes.[22, 27, 28] Hence, when the organic solvent strongly interacts with water, small angle X-ray scattering spectroscopy (SAXS) coupled with molecular dynamics (MD) simulation showed that water and organic molecules are homogeneously dispersed in the hybrid electrolyte, as observed for DMF/water mixtures. [29-32] In contrast, when the organic solvent only weakly interacts with water, aqueous and organic nanodomains co-exist in the mixtures, such as for ACN/water mixtures.[28, 33-37] As recently reported, the size and composition of these nanodomains can affect the selectivity and efficiency of electrochemical reactions,[27] including HER or CO_2 reduction[22, 38]. Similarly, the strength of the water-cation interactions was found to affect the solvation structure of these hybrid electrolytes and the selectivity of electrocatalytic reactions.[27, 28]

View Article Online
DOI: 10.1039/D5SC03012A

Despite being well documented, efforts dedicated to the optimization of reaction micro-environment, *i.e.* the liquid electrolyte composition and solvation structure, remain sparse. More specifically, the effect of water heterogeneities, their size and composition, on the outcome of electrochemical hydrogenation of unsaturated hydrocarbons remains poorly understood. In this work, we investigate how the structure of hybrid organic solvent/water electrolytes impacts the competition between the HER and electrochemical organic hydrogenation. To probe this effect, the selective hydrogenation of diphenylacetylene into Z-stilbene is studied as model reaction,[19, 20] diphenylacetylene being directly reduced at more negative potentials than water. To control the formation of aqueous heterogeneities, three organic solvents, ACN, acetone, and DMF, were selected with varying strength of interaction with water, from strong to weak, following DMF > acetone > ACN. Similarly, the proton source is varied from water to sulfuric acid. The formation of water clusters in the hybrid solution is characterized by combining Fourier-transformed infrared (FTIR) spectroscopy and synchrotron SAXS. Our results demonstrate that heterogeneities play a critical role in the outcome of the reaction, with yields greater than 80% obtained with optimized compositions. Even though the aqueous heterogeneities in ACN-based electrolyte can be modified by varying the amount of acids or solvents, the outcome of semi-hydrogenation stays low. In contrast, we find the optimum yield in DMF- and acetone-based electrolytes, showing the pivotal role of reaction environment in electrochemical semi-hydrogenation. Finally, we demonstrate that these findings are common to less oleophilic alkynes, including phenylacetylene, as well as to aldehydes which are prone to compete with the organic solvent for interacting with water.

View Article Online
DOI: 10.1039/D5SC03012A

Results and discussions

Prior to studying the effect of solvation structure on the outcome of the semi-hydrogenation of diphenylacetylene, one must first recall that water/DMF mixtures possess a negative excess enthalpy for mixing (ΔH_{mix}), indicating strong interactions between water and DMF.[27] Instead, ΔH_{mix} for water/ACN mixtures is positive, owing to the weak interactions between ACN and water molecules. Water/acetone mixtures possess a slightly positive ΔH_{mix} at low molar fraction of water, while it is negative at large molar fractions of water (> 0.5), as those studied in this work. Electrochemical study shows that this difference in strength of interaction shifts the HER potential (at current density of -2 mA.cm^{-2}) on the surface of Pt electrode towards more negative values following ACN (-1.626 V vs RHE) > acetone (-1.689 V vs RHE) > DMF (-1.995 V vs RHE) (Figure S1a), in line with our previous observations.[27] Furthermore, increasing the concentration of $LiClO_4$ from 0.1 to 1 M was found to increase the kinetics for the HER, *i.e.* to induce a shift towards more positive potential (Fig. S1b), as a result of a facilitated water dissociation step;[22, 39, 40] this effect is observed independently of the water-organic solvent interaction strength.

When adding diphenylacetylene in hybrid electrolytes containing ACN, acetone, or DMF with 5 M H_2O and different concentrations of $LiClO_4$, only traces of the product were detected after 2 hours' electrolysis at -0.8 V vs Ag/AgCl at room temperature. This finding indicates that either water does not act as proton source for hydrogenation in these conditions and/or that the HER is too fast on the surface of Pt. To disentangle both effects, similar experiments were carried out using Ni foam electrodes, previously reported to be an efficient hydrogenation electrocatalyst,[19] and no product was detected for the three solvents (Figure S6), confirming that water does not act as proton source.

DOI: 10.1039/D5SC03012A

Having established that water does not serve as proton source for semihydrogenation reaction in hybrid electrolytes, yields were measured after 2 hours' electrolysis at -0.8 V *vs* Ag/AgCl in $HClO_4/H_2O$/organic solvent mixtures, and the results are plotted for different acid concentrations and organic solvents in Figure 1b. In ACN/water mixtures (1:1, v/v), the yield is found independent of acid concentrations, and much lower than for other mixtures. By quantifying all the products formed during hydrogenation of diphenylacetylene, including both isomers formed by semihydrogenation (cis- and trans-stilbene) and dibenzyl formed by overhydrogenation, we conclude that the low conversion observed in ACN mixtures is not due to a favored overhydrogenation, the preferred formation of the second isomer (Table 1), or any other side reactions (Table S3). Fixing the applied potential to -1.1V vs RHE during the hydrogenation in 1.5M $HClO_4/H_2O$/solvent mixtures, similar results were obtained, ruling out any effect of difference in the overpotential on this process (Table S2). Moreover, results gathered using a Ni foam were compared with those obtained with a polished Ni foil under the same conditions (1.5M $HClO_4$ H_2O/solvent mixtures at -0.8V vs Ag/AgCl for 2 hours). While lower yields were obtained due to the smaller active surface area (as determined in Figure S16), similar trend to the one measured with the Ni foam was observed (Figure S3a), excluding the effect from wettability, pore access or mass transport to explain the difference measured between these three solvents.[41]

For acetone/water (1:1, v/v) and DMF/water (1:1, v/v) mixtures, the yield first increases with acid concentration before to decrease. To comprehend this trend, cyclic voltammograms were recorded to estimate the HER potential in these mixtures against the reversible hydrogen electrode (RHE) which was estimated in each solution (see Methods). When the acid concentration is fixed, the HER potential is similar in ACN-, acetone-, and DMF-based mixtures (Figure 1c and 1d). This absence of shift is due to

View Article Online
DOI: 10.1039/D5SC03012A

the fast reduction of protons when compared to water.[42-46] Proton reduction is thus not sensitive to the organic solvent, unlike water reduction for which the water dissociation step depends on the strength of the solvent molecules-water interactions. Nevertheless, the HER potential shifts to less negative potentials with acid concentrations (see Figure 1e-g and HER overpotential listed in Table S1). We therefore attribute the maximum for the yield observed in acetone/water and DMF/water mixtures when a fixed potential is applied vs Ag/AgCl, respectively at 1 M and 1.5 M of $HClO_4$, to the shift of the HER overpotential with acid concentration.[27] When increasing the acid concentration, the HER becomes faster and dominates over the semihydrogenation reaction. Finally, and to no surprise, the yield of semihydrogenation is found to decrease when decreasing the applied potential in 1.5 M $HClO_4$ DMF/water electrolyte (Figure S2), indicating that the kinetics for the semihydrogenation are dependent on potential, alike the HER.

To further confirm the trend, the reaction was carried out in a proton membrane reactor, typically used in electrochemical hydrogenation,[47-49] using the optimal reaction conditions as found above (1.5 M $HClO_4$/H_2O/solvent electrolytes and fixed applied potential of -0.8 V vs Ag/AgCl for 2 hours). When comparing the results obtained in three electrode configuration and those obtained using a proton membrane reactor, similar trends are observed with the semihydrogenation yields in ACN mixture being very low while that in acetone and DMF mixtures are much greater; one must however note that the yield recorded in DMF mixtures is slightly lower in proton membrane reactor than in the three electrode configuration (Figure S3b). We thus conclude that these differences do not arise from extrinsic factors related to the cell design.

View Article Online
DOI: 10.1039/D5SC03012A

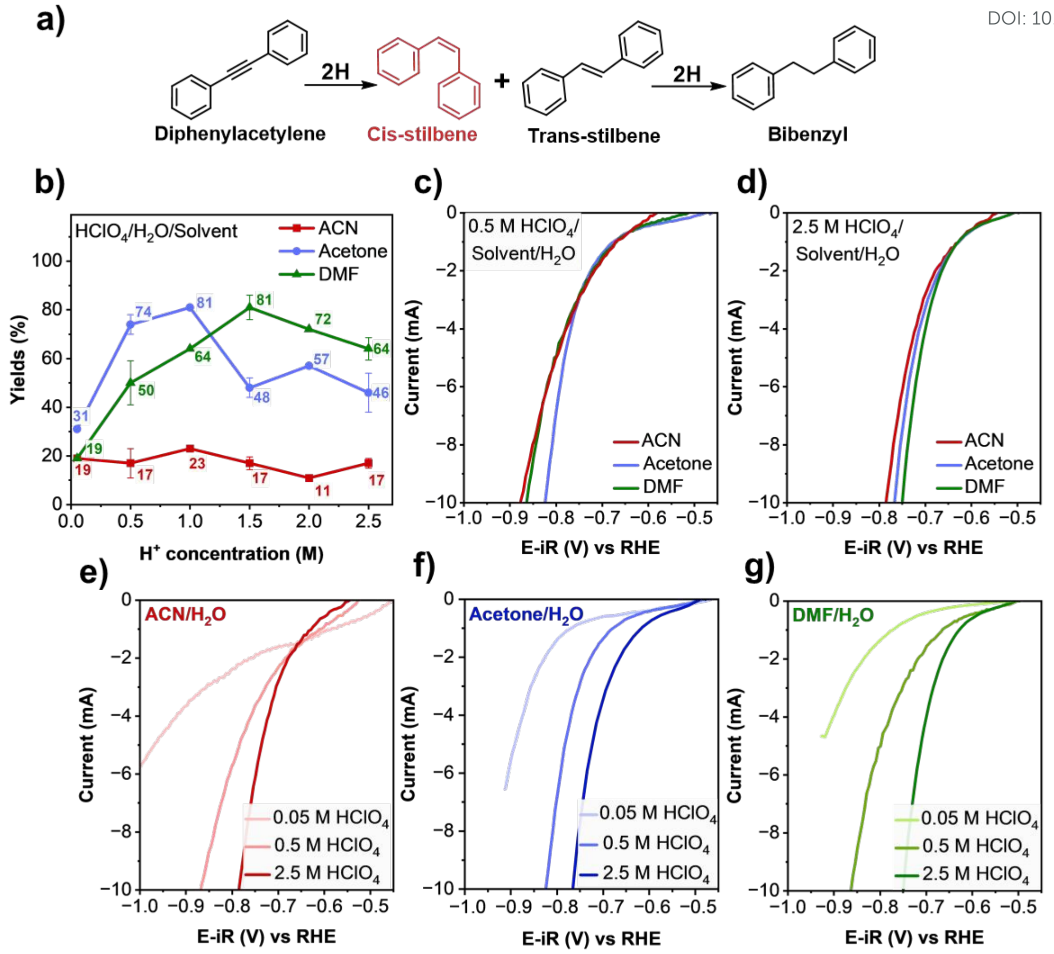

Figure 1 a) The hydrogenation processes of diphenylacetylene. b) Yields measured in hybrid electrolytes with different $HClO_4$ concentrations and organic solvents after 2 hours' electrolysis at -0.8 V *vs* Ag/AgCl. c) and d) Cyclic voltammograms recorded for hybrid electrolytes containing 0.5M and 2.5M $HClO_4$, respectively. e), f), and g) Cyclic voltammograms recorded for different $HClO_4$ concentrations in H_2O and ACN, acetone, and DMF hybrid electrolytes, respectively.

Table 1 Hydrogenation products in hybrid electrolytes at -0.8V vs Ag/AgCl for 2 hours

Hybrid electrolytes	**Selectivity (%)**			**Conversion (%)**
	Cis-stilbene 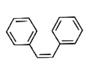	Trans-stilbene 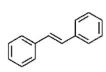	Dibenzyl 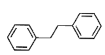	
1.5M $HClO_4/H_2O$/DMF	84	2.3	8.3	94.6
1.5M $HClO_4/H_2O$/Acetone	51	12.6	26	89.6
1.5M $HClO_4/H_2O$/ACN	14	0.8	0.6	15.4

View Article Online
DOI: 10.1039/D5SC03012A

Having established the impact of solvent, acid concentration and applied potential on the yield of semihydrogenation, we then turned our attention to the effect of water content by varying the organic solvent to water volume ratio from 1:1 to 5:1 (Figure 2a). For all the hybrid electrolytes tested in this work, the yield increases with the amount of water. This variation is not explained by a change in the HER kinetics, which remains constant in these hybrid electrolytes when varying the organic solvents or the ratio of solvent/water (Figure 2b and S8). This result indicates that the HER remains faster than the hydrogenation in these conditions and that proton reduction is not affected when varying the organic solvent/water ratio (Figure S8). Observing that water remains in large excess compared to diphenylacetylene in all the mixtures, we hypothesize that the semi-hydrogenation reaction is limited by the transport of diphenylacetylene to the interface (see discussion below). Finally, we confirmed that semi-hydrogenation is insensitive to electrolyte anion by comparing the yields obtained in perchloric and sulfuric acids, with the latter known to block the active sites for HER. Indeed, the HER potentials are found shifted to more negative potentials on Ni electrode in hybrid electrolytes containing sulfuric acid (Figure S9). Instead, for all mixtures, switching to sulfuric acid does not affect the yields when using Ni electrode (Figure S9). This difference in reactivity may indicate that the HER and the hydrogenation reaction do not share similar intermediates and/or reaction mechanism, as suggested in studies proposing that hydrogenation follows an outer-sphere reduction-protonation mechanism or an Eley-Rideal type mechanism that differ from the Volmer-Heyrosky or Volmer-Tafel HER mechanism.[50] Nevertheless, as seen in Figure S10, the cathodic current recorded using Ni foam experiences a significant shift towards more negative potential when adding diphenylacetylene in the various mixtures, which may indicate the adsorption of the substrate at the electrode. Further work, including using surface

View Article Online
DOI: 10.1039/D5SC03012A

enhanced spectroscopy techniques or computational chemistry with explicit solvent and applied potential, will be needed to clarify the exact semihydrogenation in these hybrid mixtures.

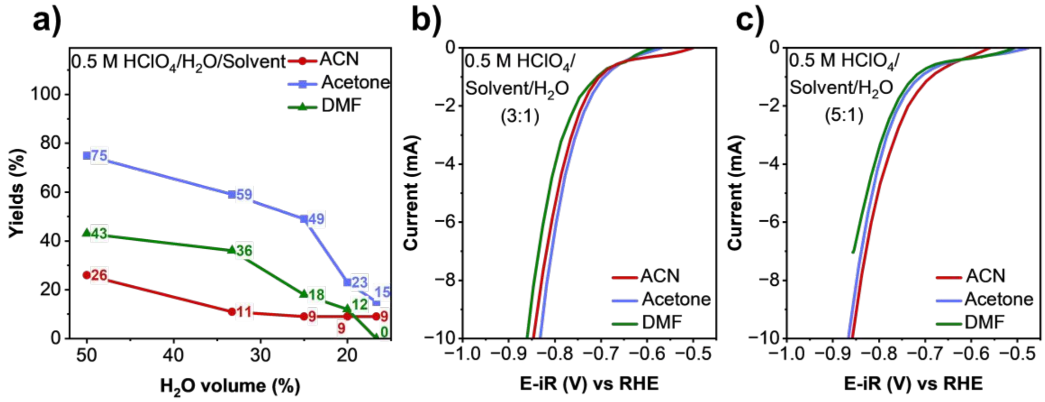

Figure 2 a) Yields in the 0.5M $HClO_4$ hybrid electrolytes with different H_2O and organic solvents compositions; b) Cyclic voltammograms recorded for hybrid electrolytes containing 0.5M $HClO_4$ with different H_2O and organic solvents compositions.

The trend measured with diphenylacetylene is also observed for the hydrogenation of other substrates, knowing that diphenylacetylene is an extremely oleophilic unsaturated organic substrate that shows very weak interaction with water. To that goal, we selected two other substrates, including another alkyne, phenylacetylene, and an aldehyde (benzaldehyde) that likely shows different interactions with water. The hydrogenation reactions were conducted in the different 1.5M $HClO_4$/H_2O/solvent electrolytes. The outcome of the phenylacetylene hydrogenation is found similar to the bulkier diphenylacetylene, with acetone and DMF providing higher yields than ACN for the semihydrogenation product (styrene), while some overhydrogenation product (ethylbenzene) was found in the various mixtures as phenylacetylene is easier to over-reduce when compared to diphenylacetylene (Figure 3a). For benzaldehyde, ACN again shows a significantly lower yield for the formation of the semihydrogenation product (benzyl alcohol) (Figure 3b). However, significantly higher yield was observed in

DOI: 10.1039/D5SC03012A

acetone mixtures compared to DMF which may be attributed to the chemical similarities existing between benzylaldehyde and acetone and their comparable ability to form hydrogen bonding with water that was previously shown to be critical for increasing the hydrogenation reaction.[51, 52]

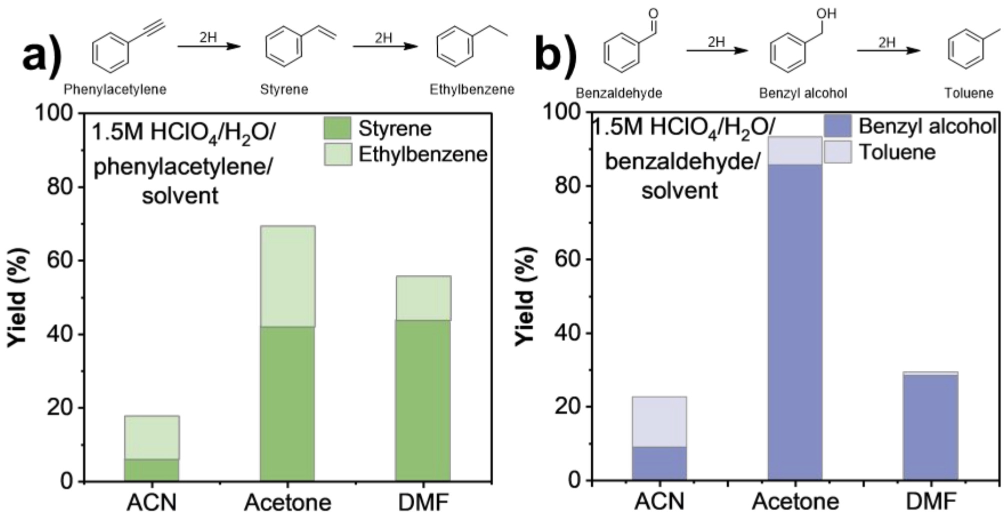

Figure 3 The yield of electrochemical semihydrogenation of a) phenylacetylene and b) benzaldehyde at -1.1V vs RHE in 1.5M $HClO_4/H_2O/DMF$ hybrid electrolytes for 2 hours using Ni foam.

One observation remains thus far unexplained, the effect of solvent on semi-hydrogenation reaction, with the yields found to increase with their strength of interaction with water. To investigate the impact of local heterogeneities on semi-hydrogenation reaction, we turned to SAXS measurements. SAXS patterns were measured with different $HClO_4$ concentrations in the q range of 0.02 to 1.2 Å^{-1} (Figure 4), where the 0.02 to 0.6 Å^{-1} q range corresponding to distances of 10.4 to 314.2 Å ($2\pi/q$) contains information regarding the growth of aqueous heterogeneities in hybrid electrolytes.[53, 54] The SAXS patterns of ACN/water mixtures show a characteristic

View Article Online
DOI: 10.1039/D5SC03012A

shape (Figure 4a-b), with scattering intensity observed in this low *q* range indicating the formation of water clusters in the mixtures owing to H_2O-H_2O and ACN-ACN self-correlation.[27, 55] Meanwhile, a relatively weak bump indicates that the heterogeneity in the acetone/water mixture is less pronounced compared to the ACN/water system. In contrast, the SAXS profile of the DMF/water mixture nearly overlaps with pure water, suggesting a high degree of miscibility between DMF and water. When increasing the acid concentration, the scattering intensity drops and the Guinier region shifts to the high *q* region, indicating a reduction in both the size and the amount of the clusters. This finding is opposite to that previously observed for strong Lewis acids such as Li^+, for which increasing the concentration was found to increase the size of the heterogeneities, owing to the strong Li^+-H_2O interactions.[22] On the contrary, as shown in Figure 4d-g, the solvation structure of acetone/water mixtures and DMF/water mixtures are independent of the amount of $HClO_4$ concentration and the water to organic solvent volume ratio. These SAXS results confirm that, as previously observed in $LiClO_4$-containing mixtures, little to no heterogeneity forms in $HClO_4$-containing acetone/water and DMF/water hybrid solution owing to the strong organic solvent-water interactions. Conversely, the heterogeneities forming in ACN/water mixtures and their size are highly sensitive to the acid concentration. Here, our results highlight that protons disrupt the hydrogen bonding network (Figure 4c). This conclusion is confirmed by observing that the scattering intensity decreases when decreasing the amount of water from 1:1 to 5:1 (v/v).

View Article Online
DOI: 10.1039/D5SC03012A

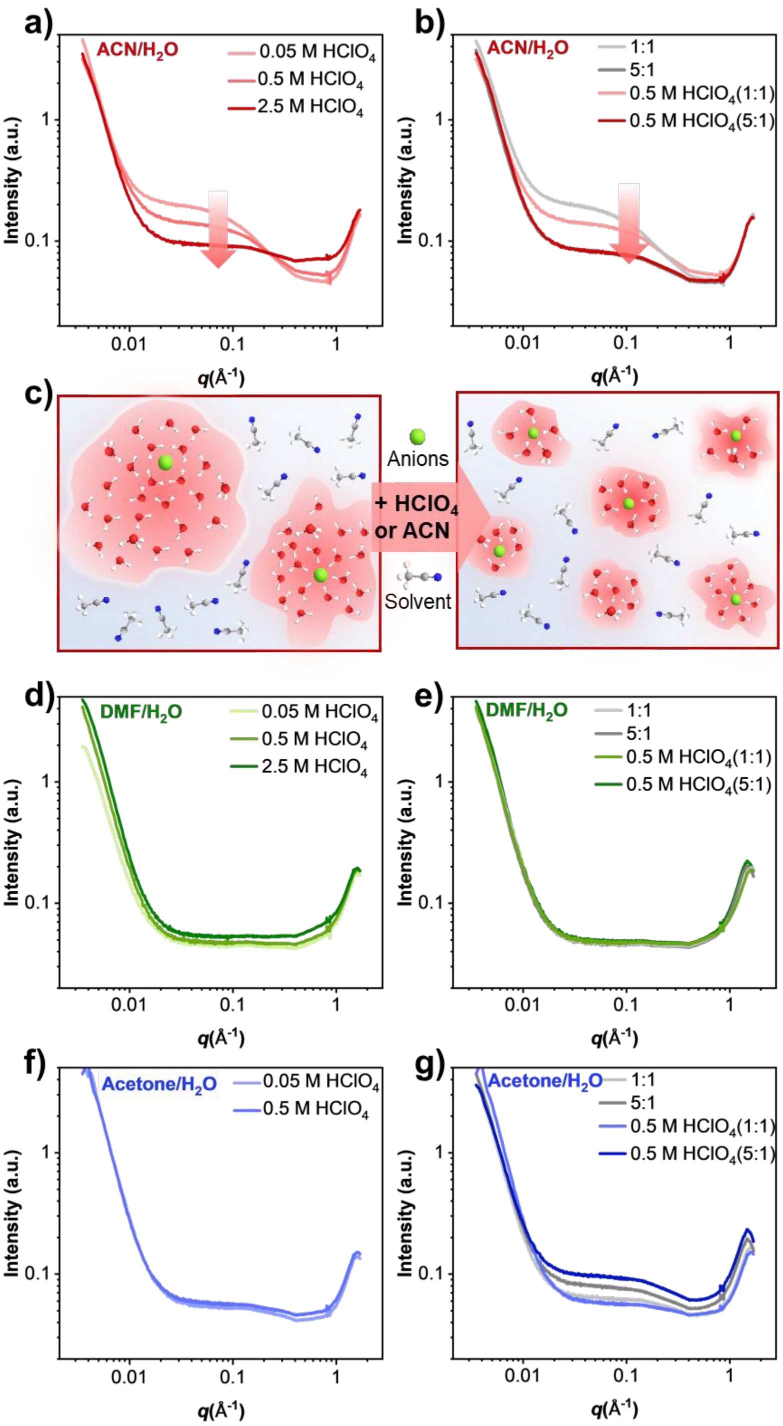

Figure 4 a) and b) SAXS spectra recorded for ACN/water with different $HClO_4$ concentrations and volume ratio of ACN and water (1:1 and 5:1), respectively. c) Scheme depicting the decrease in the size of the aqueous heterogeneities when increasing acid concentration or the ACN to H_2O volume ratio. d) and e) SAXS spectra recorded for DMF/water mixtures with different $HClO_4$ concentrations and volume ratio of DMF and water (1:1 and 5:1), respectively. f) and g) SAXS spectra recorded for acetone/water mixtures with different $HClO_4$ concentrations and volume ratio of acetone and water (1:1 and 5:1), respectively.

View Article Online
DOI: 10.1039/D5SC03012A

SAXS results were complemented by FTIR measurements to gain more insights into water environment in these mixtures (Fig. 5a-c). Looking into the OH stretching region (2800 - 3700 cm^{-1} range), a band composed of several components is observed. From previous results, one can tentatively assigned the different components to isolated water molecules (~3620 cm^{-1}), one or two H-bonded water molecules (~3540 cm^{-1}), ice-like distorted tetrahedral water networks (~3420 cm^{-1}) and ice-like water networks (~3250 cm^{-1}) (Figure 4g).[56-58] From IR spectra collected in solvent/water mixtures at different $HClO_4$ concentrations, the intensity of the contributions at ~3420 cm^{-1} and ~3250 cm^{-1} decreases in all mixtures with the addition of $HClO_4$, indicating the breaking of the hydrogen bonding network. This is accompanied by an increase in intensity for the contribution at ~3620 cm^{-1}, indicating weaker hydrogen bonding.[56] Therefore, we conclude that protons are preferentially interacting with water molecules in these electrolytes, destabilizing the water-water interactions. This hypothesis is comforted by observing that increasing the solvent to water volume ratio from 1:1 to 5:1 (Fig. 5d-f), *i.e.* decreasing the water-water interactions, decreases the intensity of the OH stretching bands in all mixtures. More precisely, the features at low wavenumber dramatically decrease, indicating the breakdown of tetrahedral water networks. Finally, by comparing the calibrated spectra for ACN/water and DMF/water mixtures (Figure S12), contributions at higher wavenumbers are found predominant in ACN mixtures with an increase in free or single paired water molecules, confirming the weaker hydrogen bonding networks in ACN-based mixtures compared to DMF ones. This conclusion is supported by observing that ΔH_{mix} for the ACN mixtures (mole fraction of water of 0.7387) is positive for the mole fractions studied in this work, while it is negative for DMF (mole fraction of 0.7987) mixtures with 0.5M $HClO_4$.[59-62] When the amount of solvent increases, ΔH_{mix} for acetone/water mixtures shifts from negative to positive,

DOI: 10.1039/D5SC03012A

explaining why acetone shows similar trend as DMF with large water amount while behaving like ACN with small water amount, as it can be seen from the IR spectra (Figure 5d and 5f).

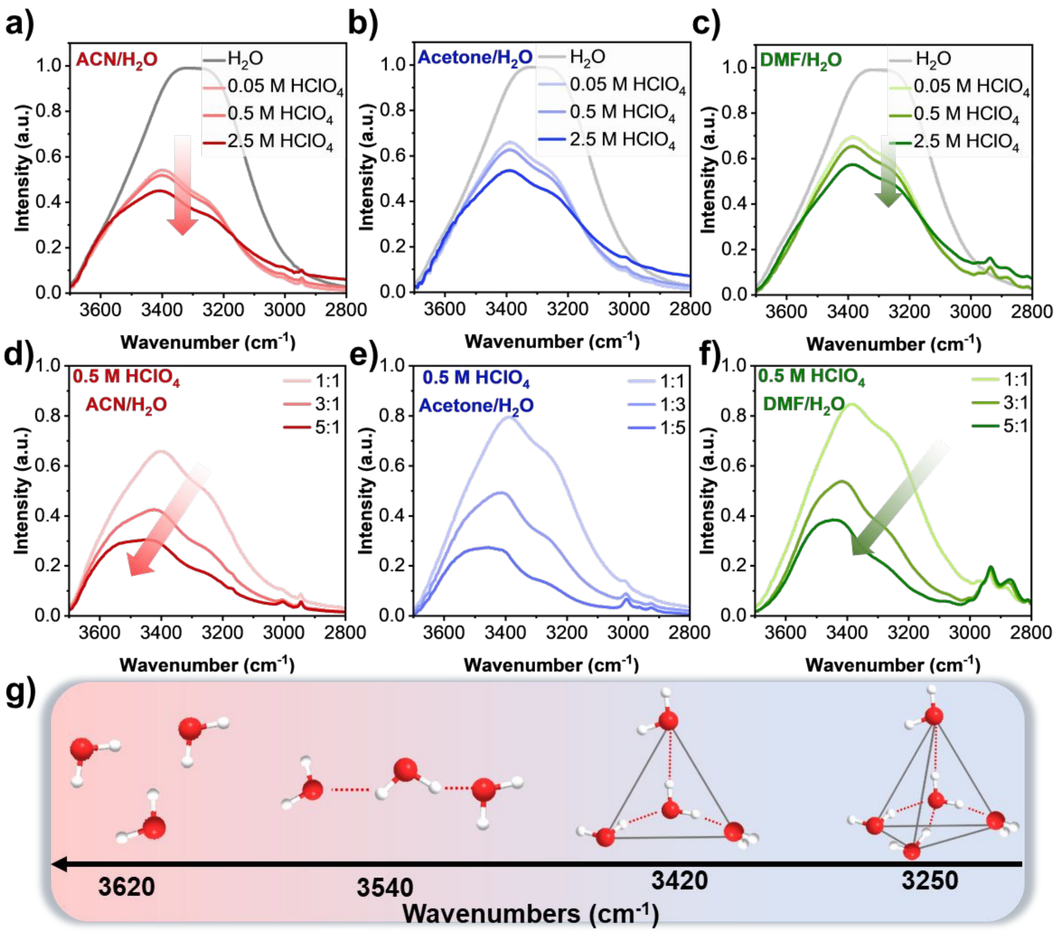

Figure 5 a), b), and c) FTIR spectra of organic solvent/water mixtures with different $HClO_4$ concentrations; d), e), and f), FTIR spectra of 0.5 M $HClO_4$ organic solvent/water mixtures with different volume ratio of solvent and water (1:1, 3:1 and 5:1); g) scheme of the change in water structures with different electrolytes' compositions.

SAXS and IR spectra have confirmed the existence of aqueous heterogeneities in ACN/water mixtures, while acetone/water and DMF/water mixtures are homogeneous. Combined with the electrochemical results, we find that the yield of electrochemical hydrogenation of unsaturated hydrocarbons (alkynes) and of one representative

View Article Online
DOI: 10.1039/D5SC03012A

aldehyde in ACN/water mixtures is always low, and we attribute this result to the presence of aqueous heterogeneities. We hypothesize that under negative polarization, the interface is rich in water, as a result of the presence of H^+ in the aqueous heterogeneities which are attracted to the interface, alike what we previously observed for Li^+-containing hybrid electrolytes.[22, 28] One can therefore conclude that a more aqueous-like interfacial solvation structure is detrimental for hydrogenation reaction (Figure 6a), likely due to the difficult access of the organic substrate to the interface which prevents its reactivity with protonated intermediates.[63] Therefore, for ACN-based mixtures, the semi-hydrogenation yield remains low independently of water or proton contents. Instead, for DMF and acetone-based systems, the electrolytes are found homogeneous. Thus, both water and the organic substrate have easier access to the interface, and the semi-hydrogenation reaction can proceed (Figure 6b). Hence, the yield in homogeneous hybrid electrolytes, *i.e.* acetone/water and DMF/water systems, is significantly higher. Moreover, the yield is affected in these systems by the acid concentration. Increasing the acid concentration increases the reactant for semi-hydrogenation and thus increases the yield, while at large concentration the HER becomes dominant, explaining the optimum observed in Figure 1b.

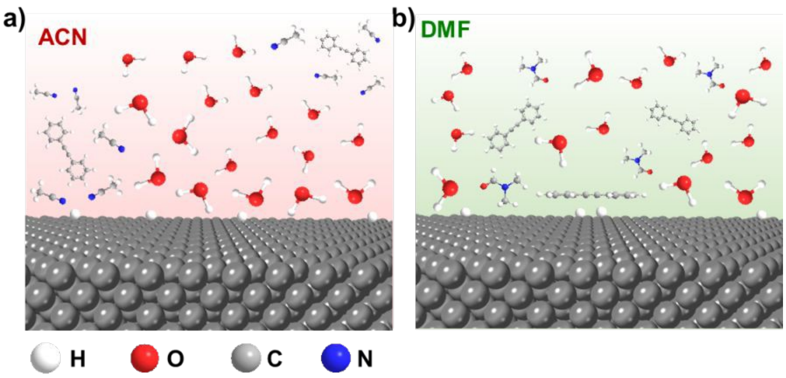

Figure 6 Scheme of interfacial environment in a) ACN-based mixtures for which the interface is rich in water due to the accumulation of aqueous domains under negative polarization while for b) DMF mixtures, the interface contains both water and the organic substrate.

View Article Online
DOI: 10.1039/D5SC03012A

Conclusion

This study demonstrates that the yield for the semi-hydrogenation of unsaturated hydrocarbons depends on the composition of the hybrid electrolytes, *i.e.* it can be tailored. First, we demonstrate that water does not serve as proton source in hybrid electrolytes for this reaction. Instead, measuring the yield for semi-hydrogenation in various electrolytes as function of acid concentration, we found that an optimum is obtained in DMF- and acetone-based mixtures with 1-1.5 M $HClO_4$. Comparing these results with the potential for the HER in these mixtures, we find that at concentrations greater than the optimum, the HER becomes predominant, while at low concentrations increasing the amount of acids increases the semi-hydrogenation yields by increasing the amount of reactants. A discrepancy is observed for ACN-based electrolyte for which the yield remains low independently of the acid concentration. Spectroscopic measurements were carried out to explain this stark difference. In ACN-based mixtures, aqueous heterogeneities were observed by SAXS, whose size decreases with increasing acid concentration and/or decreasing water content. Instead, DMF-and acetone-based electrolytes show no sign of heterogeneities (DMF) or very limited amount of heterogeneities (acetone). FTIR spectroscopic results further reveal that $HClO_4$ addition induces a weakening of the hydrogen bonding network, independently of the organic solvent; similar weakening is observed when decreasing the water content. Confronting the electrochemical results with the spectroscopic ones, we conclude that aqueous heterogeneities are detrimental for semi-hydrogenation reactions. Indeed, under negative polarization, electrochemical interface becomes rich in water for systems showing heterogeneities, as a result of the presence of H^+ in the aqueous domains. This hydrophilicity of the interface hinders the reaction by limiting the organic substrate adsorption to interact with protonated intermediates forming by H^+ reduction; the yield

View Article Online
DOI: 10.1039/D5SC03012A

thus remains low independently of the composition while the HER becomes more facile with acid concentration. This work offers the necessary understanding to tailor the reaction environment for reactions including not only hydrogenation, but also deuteration or oxygenation reactions of organic substrate that also require the use of hybrid electrolytes. Nevertheless, substantial efforts are needed in the design of electrocatalysts to increase the Faradaic efficiency (FE) and the efficiency of electrochemical semihydrogenation, which remains low due to the predominance of the HER (Figure S13). Furthermore, future work should also be dedicated to understanding the effect of substrate/water interactions, our results suggesting that it may play a significant role in the outcome of the reaction.

Experimental Section

Reagents

Acetone, acetonitrile, and dimethylformamide (HPLC grade) were purchased from Fisher Scientific. Perchloric acid (70%), diphenylacetylene, phenylacetylene, and benzaldehyde were purchased from Sigma-Aldrich. Sulfuric acid (98%) was purchased from Oakwood. D-chloroform (99.8% D) was purchased from Cambridge Isotope Laboratory. Milli-Q water (18.2 MΩ/cm at 25°C) was used for electrolytes containing water.

Electrochemical Measurements

Data were acquired on a BioLogic VSP potentiostat. All electrochemical measurements were recorded using a three-electrode cell setup with a leakless Ag/AgCl reference electrode (ET069, diameter: 5mm, L: 130mm, eDAQ) with stirring under ambient conditions. Graphite rod was used as the counter electrode and placed in a compartment separated by a frit. All electrochemical measurements were conducted at room temperature. Prior to any measurements, commercial Ni foam (from MSE) was immersed in a 0.5 M HCl solution for 5 mins to remove any oxide layer, then washed by Milli-Q water and acetone several times. The

View Article Online
DOI: 10.1039/D5SC03012A

ohmic drop was measured by electrochemical impedance spectroscopy (EIS) before and after electrochemical measurements and the values depended on the supporting salt concentration and the solvent. The ohmic drop compensation was performed in the cyclic voltammetry measurements (85% of correction).

The yield of cis-stilbene was calculated based on below equation:

$$\text{Yield (\%)} = \frac{n_{\text{cis-stilbene}}}{n_{\text{diphenylacetylene(i)}}} \times 100\% \qquad (1)$$

The Faradaic efficiency (FE) was calculated according to below equation:

$$\text{FE (\%)} = \frac{Z \times n_{\text{cis-stilbene}} \times F}{Q} \times 100\% \qquad (2)$$

Where Z is the number of electrons per molecule of the resultant product, F the Faraday constant (96,485 C/mol), Q the total charge passed in the cell during the electrolysis process (coulombs, C).

The mole balance was calculated according to below equation:[64, 65]

$$\text{Mole balance (\%)} = \frac{n_{\text{diphenylacetylene(f)}} + n_{\text{cis-stilbene}} + n_{\text{trans-stilbene}} + n_{\text{dibenzyl}}}{n_{\text{diphenylacetylene(i)}}} \times 100\% \qquad (3)$$

Where the subscripts i and f refer to the initial and final amount of diphenylacetylene.

Reversible Hydrogen Electrode (RHE) Measurements

A platinum rotating disk electrode (RDE from Pine research) rotated at 1600 rpm was used to accurately measure the RHE equilibrium potential. RHE was determined by measuring the open circuit voltage (OCV) in the H_2-saturated electrolytes using Pt RDE as working electrode, graphite rod as reference electrode. Pt electrode was polished with 0.1 μm and 0.03 μm polishing slurries and residual traces of slurries were removed by sonicating the as-polished electrodes in the water and acetone solutions three times. Polycrystalline platinum electrode was further electrochemically cleaned in 0.5 M sulfuric acid solution by 10 cycles of cyclic voltammetry (CV) between -0.25 and 1.25 V vs leakless Ag/AgCl at 50 mV/s. Then Pt electrode was rinsed by Milli-Q water and air-dried.

View Article Online
DOI: 10.1039/D5SC03012A

FTIR spectroscopy

ATR-FTIR spectra were acquired at 4cm^{-1} with 64 scans using the diamond ATR crystal on Bruker spectrometer.

Nuclear magnetic resonance spectroscopy

After 2 hours of reaction, the electrolyte was transferred into a flask and the product extracted by methylene chloride twice. The product thus collected was dissolved in d-chloroform and liquid-state ^{1}H NMR spectra were recorded at 500MHz on a Bruker AVANCE NEO spectrometer.

Small-angle X-ray scattering (SAXS)

Small-angle X-ray scattering experiments were performed at sector 12 ID-B of Advanced Photon Source at Argonne National Laboratory. A Pilatus 2M detector was located about 2m downstream from the sample. The X-ray energy is 13.3keV and exposure time is 1s. The sample-to-detector distance was calibrated using the diffraction rings of a silver behenate (AgC22H43O2) standard. The 2D scattering images collected by the detector were subsequently azimuthally averaged to 1D curves.

Acknowledgements

This work was supported by the donors of ACS Petroleum Research Fund under the grant number 67977-DNI4. This research was supported by the NSF-MRI award CHE-2117246. This work was performed at the Advanced Photon Source of Argonne National Laboratory, U.S. Department of Energy Office of Science User Facilities, and was supported by the U.S. DOE, Office of Basic Energy Sciences, under Contract No. DE-AC02-06CH11357. T. Li is thankful for the support from NSF 2323117.

References

1. Zhu, C.; Ang, N. W.; Meyer, T. H.; Qiu, Y.; Ackermann, L., Organic electrochemistry: molecular syntheses with potential. *ACS central science* **2021,** *7* (3), 415-431.

View Article Online
DOI: 10.1039/D5SC03012A

2. Jing, Q.; Moeller, K. D., From molecules to molecular surfaces. Exploiting the interplay between organic synthesis and electrochemistry. *Accounts of chemical research* **2019,** *53* (1), 135-143.
3. Frontana-Uribe, B. A.; Little, R. D.; Ibanez, J. G.; Palma, A.; Vasquez-Medrano, R., Organic electrosynthesis: a promising green methodology in organic chemistry. *Green Chemistry* **2010,** *12* (12), 2099-2119.
4. Horn, E. J.; Rosen, B. R.; Baran, P. S., Synthetic organic electrochemistry: an enabling and innately sustainable method. *ACS central science* **2016,** *2* (5), 302-308.
5. Yang, J.; Qin, H.; Yan, K.; Cheng, X.; Wen, J., Advances in electrochemical hydrogenation since 2010. *Advanced Synthesis & Catalysis* **2021,** *363* (24), 5407-5416.
6. Li, X.; Wu, X.; Tang, L.; Xie, F.; Zhang, W., Benzylamine as Hydrogen Transfer Agent: Cobalt‐Catalyzed Chemoselective C= C Bond Reduction of β‐Trifluoromethylated α, β‐Unsaturated Ketones via 1, 5‐Hydrogen Transfer. *Chemistry –An Asian Journal* **2019,** *14* (21), 3835-3839.
7. Murphy, L. J.; Ferguson, M. J.; McDonald, R.; Lumsden, M. D.; Turculet, L., Synthesis of Bis (phosphino) silyl Pincer-Supported Iron Hydrides for the Catalytic Hydrogenation of Alkenes. *Organometallics* **2018,** *37* (24), 4814-4826.
8. Tokmic, K.; Markus, C. R.; Zhu, L.; Fout, A. R., Well-defined cobalt (I) dihydrogen catalyst: experimental evidence for a Co (I)/Co (III) redox process in olefin hydrogenation. *Journal of the American Chemical Society* **2016,** *138* (36), 11907-11913.
9. Corbin, N.; Junor, G. P.; Ton, T. N.; Baker, R. J.; Manthiram, K., Toward improving the selectivity of organic halide electrocarboxylation with mechanistically informed solvent selection. *Journal of the American Chemical Society* **2023,** *145* (3), 1740-1748.
10. Li, B.; Ge, H., Highly selective electrochemical hydrogenation of alkynes: Rapid construction of mechanochromic materials. *Science Advances* **2019,** *5* (5), eaaw2774.
11. Wang, S.; Uwakwe, K.; Yu, L.; Ye, J.; Zhu, Y.; Hu, J.; Chen, R.; Zhang, Z.; Zhou, Z.; Li, J., Highly efficient ethylene production via electrocatalytic hydrogenation of acetylene under mild conditions. *Nature Communications* **2021,** *12* (1), 7072.
12. Wu, Y.; Liu, C.; Wang, C.; Yu, Y.; Shi, Y.; Zhang, B., Converting copper sulfide to copper with surface sulfur for electrocatalytic alkyne semi-hydrogenation with water. *Nature communications* **2021,** *12* (1), 3881.
13. Andrieux, C. P.; Robert, M.; Saveant, J.-M., Role of environmental factors in the dynamics of intramolecular dissociative electron transfer. Effect of solvation and ion-pairing on cleavage rates of anion radicals. *Journal of the American Chemical Society* **1995,** *117* (36), 9340-9346.
14. Han, C.; Zenner, J.; Johny, J.; Kaeffer, N.; Bordet, A.; Leitner, W., Electrocatalytic hydrogenation of alkenes with Pd/carbon nanotubes at an oil–water interface. *Nature Catalysis* **2022,** *5* (12), 1110-1119.
15. Gao, Y.; Yang, R.; Wang, C.; Liu, C.; Wu, Y.; Li, H.; Zhang, B., Field-induced reagent concentration and sulfur adsorption enable efficient electrocatalytic semihydrogenation of alkynes. *Science Advances* **2022,** *8* (8), eabm9477.
16. Chen, F.; Li, L.; Cheng, C.; Yu, Y.; Zhao, B.-H.; Zhang, B., Ethylene electrosynthesis from low-concentrated acetylene via concave-surface enriched reactant and improved mass transfer. *Nature Communications* **2024,** *15* (1), 5914.
17. Wickert, L.; Pellumbi, K.; Kleinhaus, J. T.; Wolf, J.; junge Puring, K.; Siegmund, D.; Apfel, U. P., Effect of electrolyte composition and mass transport on electrochemical hydrogenations of a terminal alkynol. *Chemie Ingenieur Technik* **2024,** *96* (5), 607-615.
18. Zhao, Y.; Wang, J.; Zha, X.; Sheng, X.; Dong, L.; Wu, X. P.; Liu, Z.; Jiang, H.; Li, C., A Cosolvent Electrolyte Boosting Electrochemical Alkynol Semihydrogenation. *J Am Chem Soc* **2025**.
19. Valiente, A.; Martínez‐Pardo, P.; Kaur, G.; Johansson, M. J.; Martín‐Matute, B.,

View Article Online
DOI: 10.1039/D5SC03012A

Electrochemical Proton Reduction over Nickel Foam for Z‐Stereoselective Semihydrogenation/deuteration of Functionalized Alkynes. *ChemSusChem* **2022,** *15* (1), e202102221.
20. Tortajada, P. J.; Kärnman, T.; Martínez-Pardo, P.; Nilsson, C.; Holmquist, H.; Johansson, M. J.; Martín-Matute, B., Electrochemical hydrogenation of alkenes over a nickel foam guided by life cycle, safety and toxicological assessments. *Green Chemistry* **2025,** *27* (1), 227-239.
21. Kolb, S.; Werz, D. B., Site‐selective Hydrogenation/Deuteration of Benzylic Olefins Enabled by Electroreduction Using Water. *Chemistry–A European Journal* **2023,** *29* (32), e202300849.
22. Dubouis, N.; Serva, A.; Berthin, R.; Jeanmairet, G.; Porcheron, B.; Salager, E.; Salanne, M.; Grimaud, A., Tuning water reduction through controlled nanoconfinement within an organic liquid matrix. *Nature Catalysis* **2020,** *3* (8), 656-663.
23. Li, P.; Guo, C.; Wang, S.; Ma, D.; Feng, T.; Wang, Y.; Qiu, Y., Facile and general electrochemical deuteration of unactivated alkyl halides. *Nature Communications* **2022,** *13* (1), 3774.
24. Norcott, P. L., Current electrochemical approaches to selective deuteration. *Chemical Communications* **2022,** *58* (18), 2944-2953.
25. Liu, C.; Chen, F.; Zhao, B.-H.; Wu, Y.; Zhang, B., Electrochemical hydrogenation and oxidation of organic species involving water. *Nature Reviews Chemistry* **2024,** *8* (4), 277-293.
26. Serva, A.; Dubouis, N.; Grimaud, A.; Salanne, M., Confining water in ionic and organic solvents to tune its adsorption and reactivity at electrified interfaces. *Accounts of Chemical Research* **2021,** *54* (4), 1034-1042.
27. Dorchies, F.; Serva, A.; Sidos, A.; Michot, L.; Deschamps, M.; Salanne, M.; Grimaud, A., Correlating Substrate Reactivity at Electrified Interfaces with the Electrolyte Structure in Synthetically Relevant Organic Solvent/Water Mixtures. *Journal of the American Chemical Society* **2024**.
28. Dorchies, F.; Serva, A.; Crevel, D.; De Freitas, J.; Kostopoulos, N.; Robert, M.; Sel, O.; Salanne, M.; Grimaud, A., Controlling the Hydrophilicity of the Electrochemical Interface to Modulate the Oxygen-Atom Transfer in Electrocatalytic Epoxidation Reactions. *J Am Chem Soc* **2022,** *144* (49), 22734-22746.
29. Koverga, V.; Juhász, Á.; Dudariev, D.; Lebedev, M.; Idrissi, A.; Jedlovszky, P., Local Structure of DMF–Water Mixtures, as Seen from Computer Simulations and Voronoi Analysis. *The Journal of Physical Chemistry B* **2022,** *126* (36), 6964-6978.
30. Liu, X.; Wang, S.; Xu, X.; Khair, H.; Dong, Z.; Wang, H.; Zhang, W.; Yu, T.; Men, Z.; Sun, C., Exploring the dynamic changes in hydrogen bond structure of water and heavy water under external perturbation of DMF. *Spectrochimica Acta Part A: Molecular and Biomolecular Spectroscopy* **2024,** *305*, 123493.
31. Tomar, D.; Rana, B.; Jena, K. C., The structure of water–DMF binary mixtures probed by linear and nonlinear vibrational spectroscopy. *The Journal of Chemical Physics* **2020,** *152* (11).
32. Venkataramanan, N. S., Cooperativity of intermolecular hydrogen bonds in microsolvated DMSO and DMF clusters: a DFT, AIM, and NCI analysis. *Journal of Molecular Modeling* **2016,** *22*, 1-11.
33. Huang, N.; Nordlund, D.; Huang, C.; Bergmann, U.; Weiss, T. M.; Pettersson, L. G.; Nilsson, A., X-ray Raman scattering provides evidence for interfacial acetonitrile-water dipole interactions in aqueous solutions. *The Journal of chemical physics* **2011,** *135* (16).
34. Marcus, Y., The structure of and interactions in binary acetonitrile+ water mixtures. *Journal of Physical Organic Chemistry* **2012,** *25* (12), 1072-1085.
35. Nagasaka, M.; Yuzawa, H.; Kosugi, N., Microheterogeneity in aqueous acetonitrile solution probed by soft x-ray absorption spectroscopy. *The Journal of Physical Chemistry B*

View Article Online
DOI: 10.1039/D5SC03012A

2020, *124* (7), 1259-1265.
36. Takamuku, T.; Noguchi, Y.; Matsugami, M.; Iwase, H.; Otomo, T.; Nagao, M., Heterogeneity of acetonitrile–water mixtures in the temperature range 279–307 K studied by small-angle neutron scattering technique. *Journal of Molecular Liquids* **2007,** *136* (1-2), 147-155.
37. Takamuku, T.; Tabata, M.; Yamaguchi, A.; Nishimoto, J.; Kumamoto, M.; Wakita, H.; Yamaguchi, T., Liquid structure of acetonitrile− water mixtures by X-ray diffraction and infrared spectroscopy. *The Journal of Physical Chemistry B* **1998,** *102* (44), 8880-8888.
38. McGregor, J.-M.; Bender, J. T.; Petersen, A. S.; Resasco, J., Organic electrolyte cations promote non-aqueous CO2reduction by mediating interfacial electric fields.
39. Cassone, G.; Creazzo, F.; Giaquinta, P. V.; Sponer, J.; Saija, F., Ionic diffusion and proton transfer in aqueous solutions of alkali metal salts. *Physical Chemistry Chemical Physics* **2017,** *19* (31), 20420-20429.
40. Liu, E.; Li, J.; Jiao, L.; Doan, H. T. T.; Liu, Z.; Zhao, Z.; Huang, Y.; Abraham, K.; Mukerjee, S.; Jia, Q., Unifying the hydrogen evolution and oxidation reactions kinetics in base by identifying the catalytic roles of hydroxyl-water-cation adducts. *Journal of the American Chemical Society* **2019,** *141* (7), 3232-3239.
41. Iwata, R.; Zhang, L.; Wilke, K. L.; Gong, S.; He, M.; Gallant, B. M.; Wang, E. N., Bubble growth and departure modes on wettable/non-wettable porous foams in alkaline water splitting. *Joule* **2021,** *5* (4), 887-900.
42. Dubouis, N.; Grimaud, A., The hydrogen evolution reaction: from material to interfacial descriptors. *Chemical Science* **2019,** *10* (40), 9165-9181.
43. Dubouis, N.; Serva, A.; Salager, E.; Deschamps, M.; Salanne, M.; Grimaud, A., The fate of water at the electrochemical interfaces: electrochemical behavior of free water versus coordinating water. *The journal of physical chemistry letters* **2018,** *9* (23), 6683-6688.
44. Suárez-Herrera, M. F.; Costa-Figueiredo, M.; Feliu, J. M., Voltammetry of basal plane platinum electrodes in acetonitrile electrolytes: effect of the presence of water. *Langmuir* **2012,** *28* (11), 5286-5294.
45. Ledezma‐Yanez, I.; Díaz‐Morales, O.; Figueiredo, M. C.; Koper, M. T., Hydrogen oxidation and hydrogen evolution on a platinum electrode in acetonitrile. *ChemElectroChem* **2015,** *2* (10), 1612-1622.
46. Ledezma-Yanez, I.; Koper, M. T., Influence of water on the hydrogen evolution reaction on a gold electrode in acetonitrile solution. *Journal of Electroanalytical Chemistry* **2017,** *793*, 18-24.
47. Nogami, S.; Shida, N.; Iguchi, S.; Nagasawa, K.; Inoue, H.; Yamanaka, I.; Mitsushima, S.; Atobe, M., Mechanistic insights into the electrocatalytic hydrogenation of alkynes on Pt–Pd electrocatalysts in a proton-exchange membrane reactor. *ACS Catalysis* **2022,** *12* (9), 5430-5440.
48. Han, G.; Li, G.; Sun, Y., Electrocatalytic hydrogenation using palladium membrane reactors. *JACS Au* **2024,** *4* (2), 328-343.
49. Sherbo, R. S.; Kurimoto, A.; Brown, C. M.; Berlinguette, C. P., Efficient electrocatalytic hydrogenation with a palladium membrane reactor. *Journal of the American Chemical Society* **2019,** *141* (19), 7815-7821.
50. Chen, H.; Iyer, J.; Liu, Y.; Krebs, S.; Deng, F.; Jentys, A.; Searles, D. J.; Haider, M. A.; Khare, R.; Lercher, J. A., Mechanism of electrocatalytic H2 evolution, carbonyl hydrogenation, and carbon–carbon coupling on Cu. *Journal of the American Chemical Society* **2024,** *146* (20), 13949-13961.
51. Cheng, G.; Jentys, A.; Gutiérrez, O. Y.; Liu, Y.; Chin, Y.-H.; Lercher, J. A., Critical role of solvent-modulated hydrogen-binding strength in the catalytic hydrogenation of benzaldehyde on palladium. *Nature Catalysis* **2021,** *4* (11), 976-985.
52. Sanyal, U.; Yuk, S. F.; Koh, K.; Lee, M. S.; Stoerzinger, K.; Zhang, D.; Meyer, L. C.;

View Article Online
DOI: 10.1039/D5SC03012A

Lopez ‐ Ruiz, J. A.; Karkamkar, A.; Holladay, J. D., Hydrogen bonding enhances the electrochemical hydrogenation of benzaldehyde in the aqueous phase. *Angewandte Chemie* **2021,** *133* (1), 294-300.
53. Liu, X.; Fang, L.; Lyu, X.; Winans, R. E.; Li, T., Unveiling the liquid electrolyte solvation structure by small angle x-ray scattering. *Chemistry of Materials* **2023,** *35* (23), 9821-9832.
54. Qian, K.; Winans, R. E.; Li, T., Insights into the nanostructure, solvation, and dynamics of liquid electrolytes through small ‐ angle x ‐ ray scattering. *Advanced Energy Materials* **2021,** *11* (4), 2002821.
55. Liu, X.; Lee, S.-C.; Seifert, S.; Winans, R. E.; Li, T., Relationship of the Molecular Structure and Transport Properties of Imide-Based Lithium Salts of "Acetonitrile/Water-in-Salt" Electrolytes. *Chemistry of Materials* **2023,** *35* (16), 6415-6422.
56. Chen, Y.; Zhang, Y.-H.; Zhao, L.-J., ATR-FTIR spectroscopic studies on aqueous LiClO4, NaClO 4, and Mg (ClO 4) 2 solutions. *Physical Chemistry Chemical Physics* **2004,** *6* (3), 537-542.
57. Khatib, R.; Backus, E. H.; Bonn, M.; Perez-Haro, M.-J.; Gaigeot, M.-P.; Sulpizi, M., Water orientation and hydrogen-bond structure at the fluorite/water interface. *Scientific reports* **2016,** *6* (1), 24287.
58. Carey, D. M.; Korenowski, G. M., Measurement of the Raman spectrum of liquid water. *The Journal of chemical physics* **1998,** *108* (7), 2669-2675.
59. Benedetti, A. V.; Cilense, M.; Vollet, D.; Montone, R., Thermodynamic properties of liquid mixtures. III. Acetone—water. *Thermochimica Acta* **1983,** *66* (1-3), 219-223.
60. Cilense, M.; Benedetti, A. V.; Vollet, D., Thermodynamic properties of liquid mixtures. II. Dimethylformamide-water. *Thermochimica Acta* **1983,** *63* (2), 151-156.
61. Morcom, K.; Smith, R., Enthalpies of mixing of water+ methyl cyanide. *The Journal of Chemical Thermodynamics* **1969,** *1* (5), 503-505.
62. Matsumoto, M.; Tanaka, H.; Nakanishi, K., Acetonitrile pair formation in aqueous solution. *The Journal of chemical physics* **1993,** *99* (9), 6935-6940.
63. Chen, B.; Wijesinghe, M. S.; Grimaud, A.; Waegele, M. M., Investigating the Electric Double-Layer Structures between a Pt Electrode and Water/Acetonitrile Hybrid Electrolytes. *The Journal of Physical Chemistry Letters* **2025,** *16* (7), 1779-1786.
64. Jung, S.; Biddinger, E. J., Electrocatalytic hydrogenation and hydrogenolysis of furfural and the impact of homogeneous side reactions of furanic compounds in acidic electrolytes. *ACS Sustainable Chemistry & Engineering* **2016,** *4* (12), 6500-6508.
65. Jung, S.; Biddinger, E. J., Controlling competitive side reactions in the electrochemical upgrading of furfural to biofuel. *Energy Technology* **2018,** *6* (7), 1370-1379.

View Article Online
DOI: 10.1039/D5SC03012A

The data supporting this article have been included as part of the Supplementary Information.